Journal of Solid State Chemistry **166,** 1–6 (2002)
doi:10.1006/jssc.2001.9499, available online at http://www/idealibrary.com on IDEAL®

A Structural Study of the Homogeneity Domain of $LaNi_5$

J.-M. Joubert,*,†,[1] R. Černý,† M. Latroche,* E. Leroy,* L. Guénée,†
A. Percheron-Guégan,* and K. Yvon†

*Laboratoire de Chimie Métallurgique des Terres Rares, CNRS, 2-8 rue Henri Dunant, 94320 Thiais, France; and †Laboratoire de Cristallographie, Université de Genève, 24 Quai Ernest Ansermet, 1211 Genève 4, Switzerland
E-mail: jean-marc.joubert@glvt-cnrs.fr

Received October 3, 2001; in revised form November 24, 2001; accepted December 21, 2001

$LaNi_5$ is a very important intermetallic compound for hydrogen storage applications. Its homogeneity range at 1200°C has been investigated by single-crystal X-ray diffraction, electron probe microanalysis, and mass density measurements. At the nickel-rich end the hexagonal structure ($CaCu_5$ type) extends to the composition $LaNi_{5.45}$. The excess of nickel is accommodated by random substitutions of lanthanum atoms by nickel dumbbells and by displacements of nickel atoms which are presumably correlated with the La atom substitutions. Interatomic distances suggest that the Ni atom displacements occur in directions toward vacant La atom sites, i.e., toward the center of Ni dumbbells. At the nickel-poor end the structure extends to the composition $LaNi_{4.88}$. The excess of lanthanum is presumably accommodated by the simultaneous occurrence of lanthanum atoms and vacancies on nickel atom sites. Both models are consistent with mass density and electron probe microanalysis measurements. Hydrogenation thermodynamic properties have been measured as a function of composition.

Key Words: **intermetallics; hydrides; $LaNi_5$; crystal structure; EPMA; nonstoichiometry.**

INTRODUCTION

The intermetallic compound $LaNi_5$ (hexagonal, $CaCu_5$ structure type) and its substitutional derivatives AB_{5+x} (A = rare earth, B = d- and p-block elements) continue to be the subject of major interest because of their favorable hydrogen storage properties and their use in rechargeable metal hydride batteries (1). A most important parameter is the compositional ratio B/A in as much as it controls properties such as plateau pressure and cycle life (2, 3). For binary $LaNi_{5+x}$ past investigations have suggested (4) that the phase extends over the compositional range $-0.15 \leq x \leq 0.40$ at a temperature of 1200°C. At lower temperatures this range becomes more narrow and nearly vanishes at the stoichiometric composition $LaNi_5$ around 1000°C. As to its crystal structure no systematic study as a function of x has been reported as yet. For superstoichiometric compositions ($x>0$) the increase of the cell axis ratio c/a as a function of x has been interpreted as the result of random substitutions of La by Ni dumbbells in analogy with the corresponding compositions in the Sm–Co system (4). Experimental support for the dumbbell model in the La–Ni system has been reported first by Latroche *et al.* (5), who investigated an alloy of composition $LaNi_{5.4}$ by a joint neutron and synchrotron powder diffraction study. For substoichiometric compositions ($x<0$) the variations of cell parameters have been interpreted as random substitutions of Ni by La in analogy with La_2Ni_7 whose structure can be derived from $LaNi_5$ by ordered substitutions of Ni by La (4). The aim of the present work was to investigate the $LaNi_{5+x}$ phase over the entire compositional range by single-crystal X-ray diffraction and to correlate the results with carefully measured compositions, mass densities, and thermodynamic properties such as hydrogen absorption plateau pressures, this latter parameter being very sensitive to cell volume variation.

EXPERIMENTAL

Eight alloys of various compositions were synthesized by induction melting of the elements. Six of them were inside or close to the limits of the homogeneity range of the $LaNi_{5+x}$ phase as given in Ref. (4) and had the molar ratios Ni/La = 4.8, 4.85, 5, 5.2, and 5.4. Two of them were in two-phase regions such that their nominal compositions $La_{10}Ni_{90}$ and $La_{20}Ni_{80}$ made it possible to assess the Ni-rich and -poor phase limits, respectively. All alloys were annealed at 1200°C except for stoichiometric $LaNi_5$, which was annealed at 1100°C. For the La-rich alloy $La_{20}Ni_{80}$ annealing at 1200°C leads to segregation into a solid and a

[1]To whom correspondence should be addressed. Present address is the Laboratoire de Chimie Métallurgique des Terres Rares.

0022-4596/02 $35.00

liquid part, in agreement with the binary phase diagram (6). Segregation due to gravity occurs while annealing and a major part of the solid resulting from the crystallization can be separated and put aside. According to the phase diagram, this preparation method makes it possible to recover Ni-poorest $LaNi_{5+x}$ together with additional phases resulting from the crystallization of the remaining liquid, but in rather small quantities. Despite the fact that the nominal composition of that sample has changed it is still designated "$La_{20}Ni_{80}$."

Powder X-ray diffraction (XRD) patterns were recorded on a laboratory source and analyzed by the Rietveld method in order to derive cell parameters and the concentration of secondary phases, if present. Mass density measurements were performed by using a gas pycnometer (Micromeritics Accupic 1330). In order to evaluate the concentration dependence of the hydrogen sorption properties *P–C–T* curves were measured during both absorption and desorption at 40°C by using the Sievert method, and so-called plateau pressures are defined as the pressure at half the total capacity. Electron probe microanalysis (EPMA) (CAMECA SX100) using the wavelength dispersive spectroscopy method was used to check the homogeneity of the alloys, to identify the nature of additional phases, if any, and to measure accurate stoichiometry of the main phase. For La quantification, the use of pure La is prohibited by the strong oxidation of this element. Therefore, the use of an intermetallic compound such as $LaAl_2$ or, better, $LaNi_5$ is preferable. In addition, if the Ni quantification is done with pure Ni, a deficiency is observed, resulting in a sum of analyzed concentrations of only 98 wt%. This could be caused by an uncorrected matrix effect, not observed, for example, in the case of Cu analysis in $LaCu_5$. Therefore, in order to obtain reliable measurements, a reference alloy must be used for the quantification. It was elaborated at the nominal composition $LaNi_5$ and carefully checked to be absolutely single phase by metallographic and X-ray analyses. With the assumption of being absolutely single phase, the ion-coupled plasma (ICP) method, which gives reliable macroscopic elementary analysis of the sample, was used to measure the actual composition of the $CaCu_5$-type phase. The result obtained is $LaNi_{4.97(5)}$ in perfect agreement with the nominal stoichiometry. This sample was used as a reference for the EPMA analyses of both La and Ni elements in the other samples. For the single-crystal diffraction experiments small single crystals (parallelepipeds with edge lengths of up to 60 μm) were isolated from the crushed alloys and mounted on a Philips PW1100 and Enraf-Nonius CAD 4 four-circle diffractometer ($MoK\alpha_1$ radiation, theta range 0°–30°, equivalent reflections averaged over full or half of the reciprocal space yielding 73 unique reflections; analytical absorption correction). All reflections could be indexed on the known hexagonal structure. No superstructure peaks were found. Various structure models based on the $CaCu_5$-type structure (space group *P6/mmm*: $Z = 1$, La in 1*a* (0, 0, 0); Ni in 2*c* ($\frac{1}{3}$, $\frac{2}{3}$, 0); Ni in 3*g* ($\frac{1}{2}$, 0, $\frac{1}{2}$)) were refined on *F* by using XTAL 3.2 (7) (see below). Secondary extinction was refined according to Becker and Coppens (8) by assuming a Gaussian distribution of the mosaic blocks. Diffuse intensity was not analyzed.

RESULTS

The results obtained for the various samples are summarized in Table 1. None of the samples contained significant amounts of secondary phases in addition to the $LaNi_{5+x}$ phase except lanthanum-rich $La_{20}Ni_{80}$, which also contained La_2Ni_3, La_7Ni_{16}, and $LaNi_3$, and nickel-rich $La_{10}Ni_{90}$, which also contained a significant amount of *fcc* Ni solid solution. The cell parameters of $LaNi_{5+x}$ are plotted in Fig. 1. For superstoichiometric compositions *c* increases while *a* (and *V*) decreases as a function of *x* as has been reported before (4). This trend is consistent with a model in which La atoms are substituted by Ni dumbbells oriented along *c*. Given the absence of superstructure reflections the substitutions are presumably random. For substoichiometric compositions the cell parameters do not change much between $LaNi_5$, $LaNi_{4.85}$, $LaNi_{4.8}$, and $La_{20}Ni_{80}$.

The measured densities of the $LaNi_{5+x}$ phase are plotted in Fig. 2. That in $La_{20}Ni_{80}$ was corrected for the presence of La_2Ni_3 (1.5 wt%, 7.7 g.cm^{-3}), La_7Ni_{16} (3.4 wt%, 8 g.cm^{-3}), and $LaNi_3$ (4.1 wt.%, 8.4 g.cm^{-3}). In view of the small quantities involved and the small density difference with respect to the main phase (8.2 g.cm^{-3}) the correction is not very important. The density of the $LaNi_{5+x}$ phase in $La_{10}Ni_{90}$ was not estimated in view of the uncertainties due to the relatively large amount (30 wt%) of *fcc* phase present. The measured densities were compared with those calculated on the basis of various structure models. For superstoichiometric compositions three structure models were considered (see lines in Fig. 2): vacancy model (La vacancies), dumbbell model (2 Ni for 1 La), and substitution model (1 Ni for 1 La), and for substoichiometric compositions two models: vacancy model (Ni vacancies) and substitution model (1 La for 1 Ni). Clearly, for superstoichiometric compositions the dumbbell model shows the best agreement with the experimental data, while for substoichiometric compositions the relatively constant measured density seems to preclude a significant concentration of Ni vacancies.

The concentration dependence of the hydrogen absorption and desorption plateau pressures is plotted in Fig. 3. Three domains can be distinguished, two (those at low and high Ni contents) having relatively constant plateau pressures, and one (that in the central part) having a

TABLE 1
Summary of the Results Obtained on the Different Samples

Nominal composition	Alloy number	Heat treatment	Analyzed composition	a(Å)	c(Å)	V(Å^3)	Density (g.cm^{-3})	Refined composition	Absorption pressure (40°C) (bar)	Desorption pressure (40°C) (bar)
"$La_{20}Ni_{80}$"[a]	1	96 h, 1200°C	$LaNi_{4.88(2)}$	5.0219(1)	3.9812(1)	86.955(6)	8.262(5)[b]	Not refined	3.92	3.12
$LaNi_{4.8}$	2	5 h, 1200°C	$LaNi_{4.90(4)}$	5.0189(2)	3.9795(2)	86.812(5)	8.290(6)	Not refined	4.15	3.25
$LaNi_{4.85}$	3	96 h, 1200°C	$LaNi_{4.87(4)}$	5.0192(10)	3.9795(11)	86.820(40)	8.310(4)	Not refined	4.07	2.89
$LaNi_5$ (ref. sample)	4	3.5 h, 1100°C	$LaNi_{4.97(5)}$ (ICP)	5.0177(1)	3.9811(1)	86.805(4)	8.310(2)	Not refined	4.0	3.45
$LaNi_{5.2}$	5	96 h, 1200°C	$LaNi_{5.11(11)}$	5.0050(1)	3.9890(1)	86.536(4)	8.332(7)	5.19(2)	6.37	4.98
$LaNi_{5.4}$	6	96 h, 1200°C	$LaNi_{5.44(5)}$	4.9955(2)	3.9987(2)	86.417(5)	8.298(7)	5.42(2)	9.81	7.32
$LaNi_{5.4}$	7	96 h, 1200°C	$LaNi_{5.52(7)}$	4.9922(1)	3.9991(1)	86.313(2)	8.342(5)	5.53(2)	10.23	7.73
$La_{10}Ni_{90}$[c]	8	96 h, 1200°C	$LaNi_{5.43(5)}$	4.9933(1)	3.9998(1)	86.367(4)	—	5.46(3)	9.60	7.70

Note. The nominal composition, the heat treatment, the analyzed composition by EPMA (except for $LaNi_5$), the lattice parameters obtained by powder XRD, the measured density, the composition as refined from single-crystal data, and the hydrogen absorption and desorption plateau pressures at 40°C are given.
[a]Due to segregation of the liquid phase, the actual composition is different from the nominal composition indicated.
[b]The measured density for the multiphase alloy has been corrected for the presence of additional phases.
[c]The data corresponding to this alloy refer to the $CaCu_5$-type phase present solely in the amount of 70 wt%.

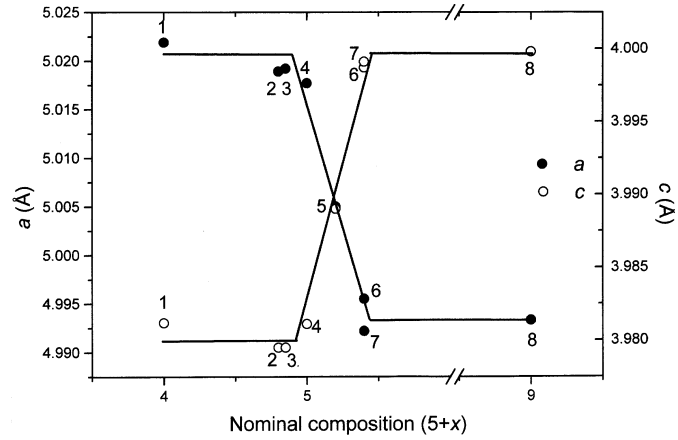

FIG. 1. Lattice parameters a and c obtained by powder XRD as a function of the nominal composition for $LaNi_{5+x}$ phases.

plateau pressure that increases with Ni content. As pointed out by Achard *et al.* (9), the pressure variation in the latter regime as a function of composition and cell volume is linear on a logarithmic scale.

The single-crystal X-ray data on stoichiometric $LaNi_5$ confirmed the fully ordered $CaCu_5$-type structure (goodness of fit $S = 1.76$, $R_F2 = 3.6\%$). For superstoichiometric $LaNi_{5+x}$ a preliminary structure refinement based on the stoichiometric model and data of a crystal isolated from Ni-rich $La_{10}Ni_{90}$ yielded electron density difference maps as shown in Fig. 4. The positive peaks in the prismatic plane (those at 0, 0, $z \approx 0.30$) suggested that a significant fraction of La atoms (site 1*a*) was substituted by Ni dumbbells oriented along c (site 2*e*). Subsequently, a

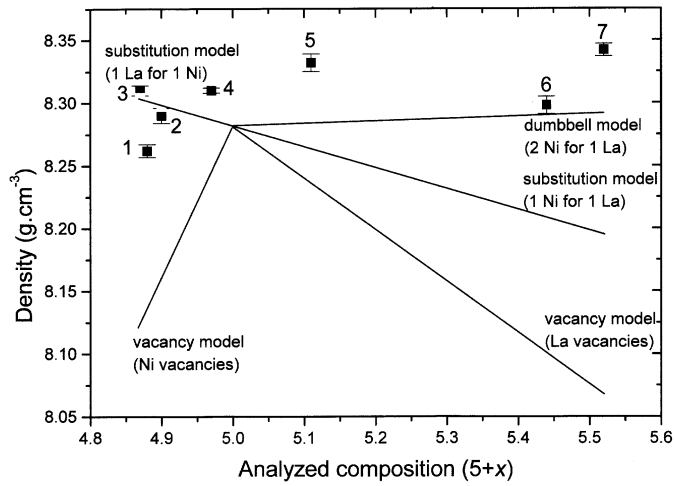

FIG. 2. Measured density as a function of the analyzed composition for $LaNi_{5+x}$ phases in samples 1–7 (see Table 1, squares). The density of the $La_{20}Ni_{80}$ sample has been corrected for the presence of the additional phases. Lines refer to calculated densities according to different models able to explain the nonstoichiometry as indicated in the figure.

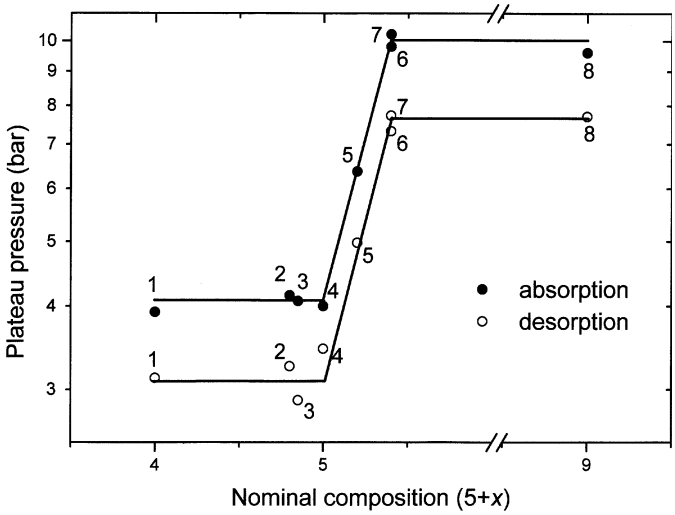

FIG. 3. Absorption and desorption plateau pressures at 40°C as a function of the nominal composition for $LaNi_{5+x}$ phases. Note logarithmic scale of plateau pressure.

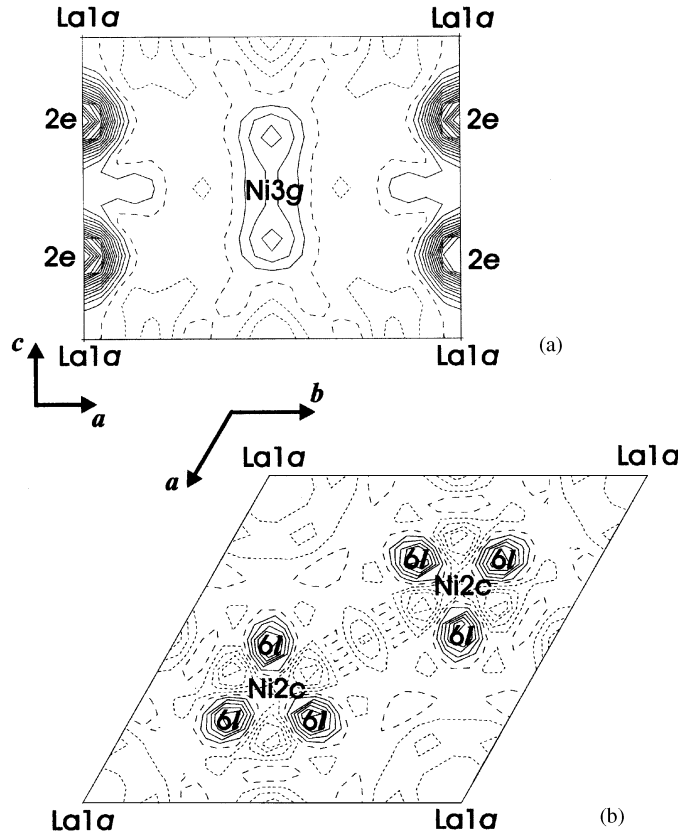

FIG. 4. Difference Fourier maps of the $CaCu_5$-type phase present in the $La_{10}Ni_{90}$ alloy (sample 8) (analyzed composition of the phase $LaNi_{5.43}$) refined with the stoichiometric $CaCu_5$-type model in the prismatic (110) (a) and basal (001) (b) planes of the hexagonal cell (the zero density contour is dashed, peaks are represented by full lines, holes by dotted lines, contours are drawn at $0.5\,e^-/Å^3$ intervals).

refinement based on this assumption was performed, in which Ni atoms on sites 2*c* were fixed. It converged at $R_F2 = 3.1\%$ and $S = 1.98$, and yielded highly anisotropic harmonic displacement parameters for position 2*c*. In a second refinement, and according to the positive peaks shown in Fig. 4b, an appropriate fraction of them was allowed to relax toward the missing La atoms, i.e., on site 6*l* (disordered model, see Discussion). In this second refinement the following constraints were introduced to obtain convergence. Each vacant La site was assumed to be occupied by one Ni dumbbell and to generate displacements of six nearest Ni atoms from site 2*c* toward site 6*l*. With that scheme only one parameter, *s*, was refined, corresponding to the following occupancy factors: 1*a*:1-*s*; 2*c*:1-3*s*; 3*g*:1; 2*e*:*s*; 6*l*:*s*, and the following compositions: $La_{1-s}Ni_{5+2s}$ and $LaNi_{(5+2s)/(1-s)}$ (normalized to one La atom). The refinement converged at $R_F2 = 2.5\%$ and $S = 1.92$; i.e., it yielded an agreement better than that of the previous model. Complete refinement results of that model are summarized in Table 2. The same model was also used for all other superstoichiometric crystals. As shown in Table 1 the refined compositions are in good agreement with those analyzed. In particular, those obtained on the Ni-rich sample $La_{10}Ni_{90}$ suggest the limit to be $LaNi_{5.45}$, which is in good agreement with previous results (4).

For substoichiometric crystals ($x<0$) the structure refinements were less straightforward. For $La_{20}Ni_{80}$ the refined Ni occupancies of sites 2*c* (1.980(8)/2) and 3*g* (3.00(2)/3) and the resulting composition ($LaNi_{4.98(3)}$) did not differ significantly from those corresponding to full occupancy, while the fits (occupancy refined: $S = 1.82$, $R_F2 = 2.2\%$; full occupancy: $S = 1.84$, $R_F2 = 2.2\%$) were practically identical. This excludes the possibility of nickel being substituted solely by lanthanum since this would result in a significant increase of electron density at these sites and thus in an inferior fit to the data. On the other hand, refinements under the assumption of Ni vacancies

TABLE 2

Single-Crystal Refinement of the $CaCu_5$-Type Phase Present in the $La_{10}Ni_{90}$ Alloy (Sample 8) (Analyzed Composition of the Phase $LaNi_{5.43}$)

Atom	Site	*x*	*y*	*z*	U_{eq}
La	1*a*	0	0	0	0.0098(1)
Ni	2*c*	$\frac{1}{3}$	$\frac{2}{3}$	0	0.0097(4)
Ni	3*g*	$\frac{1}{2}$	0	$\frac{1}{2}$	0.0088(2)
Ni	2*e*	0	0	0.276(2)	0.013(3)
Ni	6*l*	0.289(1)	2*x*	0	0.004(2)
s	0.070(3)				

Note. Occupancy factors are set as follows: 1*a*:1-*s*; 2*c*:1-3*s*; 3*g*:1; 2*e*:*s*; 6*l*:*s*, refined composition : $LaNi_{5.46(3)}$, Goodness-of-fit $S = 1.92$, $R_F2 = 2.5\%$.

lead to agreement factors slightly, but not significantly, better than those of the stoichiometric model, but the results were at variance with the composition as measured by EPMA ($LaNi_{4.88(2)}$).

DISCUSSION

Since constant plateau pressures and cell parameters indicate a constant composition of the absorbing phase they make it possible to assess the homogeneity range of the $LaNi_{5+x}$ phase. Figures 1 and 3 are therefore in agreement with the EPMA results, indicating a homogeneity domain from $LaNi_{4.88}$ to $LaNi_{5.45}$. The hydrogenation measurements are consistent with those reported in (4).

For superstoichiometric $LaNi_{5+x}$ the present work confirms a structural model in which La atoms are partially substituted by Ni dumbbells, and part of the Ni atoms are displaced in directions toward empty La sites (see below). The model is consistent with nominal compositions, analyzed compositions, and the mass density measurements. The presence of dumbbells in $CaCu_5$-type structures have been originally proposed by Buschow and Van der Goot (10) for superstoichiometric $SmCo_{5+x}$ in their attempt to explain the concentration dependence of the cell parameters of that phase by comparison with structurally related Sm_2Co_{17}. The presence of dumbbells was further investigated by Schweizer and Tasset (11), who compared observed and calculated powder diffraction intensities for various models of $ErCo_{5+x}$. A model of correlated *B* atom displacements (i.e., a shrinkage of *B* atom hexagons in the immediate vicinity of vacant *A* atom sites) was first proposed by Hornstra and Buschow for $YbCu_{6.5}$ (12), although no structure refinement has been performed. To our knowledge, the first complete structure refinement on AB_{5+x}-type compounds yielding both the dumbbell substitution ratio and the fraction of B atoms displaced from site 2*c* to site 6*l* was performed by Givord *et al.* (13) by single-crystal neutron diffraction on $SmCo_5$. However, disagreement was obtained between nominal ($SmCo_5$) and refined ($SmCo_{5.22}$) compositions.

The present work on hyperstoichiometric $LaNi_{5+x}$ confirms the above structure model and for the first time provides complete agreement between structural parameters such as dumbbell substitution ratios and fractions of displaced atoms, and independent measurements of composition and mass density. The model involves four distinctly different Ni sites, of which one (2*c*) is partially, and two (6*l*, 2*e*) are fully disordered. Among the latter, site 6*l* is of particular interest because its occupancy on the local level is likely to be correlated with the occurrence of a defect on a neighbouring La site, as observed in related 2:17 structures where this displacement is ordered (14). Moreover, interatomic distances suggest that the local Ni atom displacements should occur in directions toward vacant La atom sites (closest distance toward two occupied La sites: Ni–La = 3.14(1) Å) rather than away from them (closest distance towards one occupied La site: Ni–La = 2.41(1) Å). However, proof for this correlation and the associated local structural features must await the analysis of diffuse scattering intensity. In any case, modeling of the electron density in terms of anisotropic (harmonic) potentials centered on site 2*c* as suggested by Daams and Villars (15) or adopted experimentally by Vogt *et al.* (16) in the refinement of $La(Ni,Sn)_{5+x}$ where the occupancy of both sites 2*e* and 6*l* has been modeled by large anisotropic (harmonic) thermal displacement amplitudes centered on sites 1*a* and 2*c* should be avoided.

For substoichiometric $LaNi_{5+x}$ the microprobe analysis of the segregated $La_{20}Ni_{80}$ alloy indicates the lower phase limit to be $LaNi_{4.88(2)}$. The same limit has been found for the $CaCu_5$-type phase in the Y–Co system (17). Two structure models were initially considered to account for the Ni deficiency, Ni vacancies, and substitution of Ni by La. While the first model leads to a rather small vacancy concentration (not more than 0.02 Ni vacancy per formula unit) and is not consistent with mass density measurements (calculated value $\sim$8.15 (to account for a composition of $LaNi_{4.88}$) as compared to a measured value of 8.26), the second model can be excluded on diffraction grounds. Thus, a third model based on the simultaneous occurrence of lanthanum atoms and vacancies on nickel atom sites was considered. In fact, given the electron number and molar weight of Ni (28, 58.7) and La (57, 138.9), such a model changes only little the electron density and the mass density compared to those of the stoichiometric phase, which is observed, while it explains the Ni deficiency as measured by EPMA. From atomic size considerations substitution of Ni by La should be accompanied by the creation of vacancies at neighboring Ni sites because of spatial hindrance, therefore leading to relatively constant cell parameters in this region, which is observed. It is not possible, from a single diffraction data set, to refine simultaneously vacancy and La substitution on the same site. It is possible, however, to check the consistency of the diffraction data against structure models that involve double defects on one or both nickel sites. All of them (e.g., $LaNi_2(Ni_{0.982(2)}La_{0.0045(4)}\square_{0.0135(20)})_3$, $S = 1.82$, $R_F2 = 2.2\%$, constrained to the composition $LaNi_{4.88}$, calculated density 8.24) lead to the same agreement factors as those obtained for the vacancy model while explaining both the measured composition and the experimental density.

ACKNOWLEDGMENTS

The authors thank L. Touron, F. Demany, F. Briaucourt, and V. Lalanne from the Laboratoire de Chimie Métallurgique des Terres Rares for technical assistance. The ICP measurement was done by J.-C.

Rouchaud of the Centre d'Etudes de Chimie Métallurgique of the CNRS in Vitry. This work was supported by the Swiss National Science Foundation and the Swiss Federal Office of Energy.

REFERENCES

1. F. Cuevas, J.-M. Joubert, M. Latroche, and A. Percheron-Guégan, *Appl. Phys. A* **72,** 225–238 (2001), doi:10.1007/s003390100775.
2. P. H. L. Notten, R. E. F. Einerhand, and J. L. C. Daams, *J. Alloys Compd.* **210,** 221–232 (1994).
3. P. H. L. Notten, J. L. C. Daams, and R. E. F. Einerhand, *J. Alloys Compd.* **210,** 233–241 (1994).
4. K. H. J. Buschow and H. H. Van Mal, *J. Less-Common Met.* **29,** 203–210 (1972).
5. M. Latroche, J.-M. Joubert, A. Percheron-Guégan, and P. H. L. Notten, *J. Solid State Chem.* **146,** 313–321 (1999), doi:jssc.1999.8348.
6. H. Okamoto, *J. Phase Equilibria* **12,** 615–616 (1991).
7. S. R. Hall, H. D. Flack, and J. M. Stewart (Eds.), "XTAL 3.2 Reference Manual." Universities of Western Australia, Geneva and Maryland, Lamb, Perth, 1992.
8. P. J. Becker and P. Coppens, *Acta Crystallogr. Sect. A* **30,** 148 (1974).
9. J.-C. Achard, A. Percheron-Guégan, H. Diaz, F. Briaucourt, and F. Demany, *in* "Proc. 2nd Int. Congr. on Hydrogen in Metals," Paris, p. 1E12, 1977.
10. K. H. J. Buschow and A. S. Van der Goot, *J. Less-Common Met.* **14,** 323–328 (1968).
11. J. Schweizer and F. Tasset, *J. Less-Common Met.* **18,** 245–250 (1969).
12. J. Hornstra and K. H. J. Buschow, *J. Less-Common Met.* **27,** 123–127 (1972).
13. D. Givord, J. Laforest, J. Schweizer, and F. Tasset, *J. Appl. Phys.* **50**(3), 2008–2010 (1979).
14. Y. Ono, J. Shiomi, H. Kato, T. Iriyama, and T. Kajitani, *J. Magn. Magn. Mater.* **187,** 113–116 (1998).
15. J. L. C. Daams and P. Villars, *J. Alloys Compd.* **215,** 1–34 (1994).
16. T. Vogt, J. J. Reilly, J. R. Johnson, G. D. Adzic, and J. McBreen, *Electrochem. Solid State Lett.* **2**(3), 111–114 (1999).
17. Chang Heng Wu, Yu Chi Chuang, and Xu Ping Su, *Z. Metallkd.* **82,** 73–79 (1991).